Impact Factor (SJIF): 6.092 E-ISSN: 2583-1615

International Journal of Research in Academic World

Received: 03/November/2024 IJRAW: 2024; 3(12):36-46 Accepted: 07/December/2024

Photocatalysis for Environmental Remediation and Energy Applications: An Overview

[1]Tejveer Singh Tanwer, [2]Jinesh Menaria, [3]Dushyant Kumar Prajapati, [4]Jeevan Kunwar Chouhan and *[5]Shipra Bhardwaj

[1, 2, 3, 4]Research Scholar, Department of Chemistry, Government Meera Girls College, Mohan Lal Sukhadia University, Udaipur, Rajasthan, India.

*[5]Professor, Department of Chemistry, Government Meera Girls College, Mohan Lal Sukhadia University, Udaipur, Rajasthan, India.

Abstract

Photocatalysis is a promising technology for environmental remediation and energy applications, where photocatalyst uses light energy to drive chemical reactions. The process involves excitation of electrons creating electron-hole pairs, that facilitate oxidation and reduction reactions. Key factors affecting photocatalytic performance include band gap energy, light intensity, catalyst loading, pH, reactant concentration etc. Photocatalysts are classified into types such as traditional metal oxides (e.g., TiO_2, ZnO), metal sulfides, graphene-based materials, plasmonic photocatalysts etc., each with unique properties and applications. The review emphasizes their use in degrading organic pollutants, removing heavy metals, water splitting etc., with a focus on advanced oxidation processes for enhanced pollutant degradation and wastewater treatment.

Keywords: Photocatalysis, photodegradation, organic and inorganic pollutant, wastewater treatment, advance oxidation process.

1. Introduction

Industrialization, technologies and consumption of nonrenewable sources are increasing at a rapid rate since the last few decades because of continuous increasing demands of materials related to textile, dye, fertilizer, domestic, plastic etc. As a consequence environmental pollution and energy crises have already reached an alarming stage. The industrial wastes are more toxic and non-biodegradable as compared to municipal wastes because these consist of fats, oil, grease, heavy metals, phenols, ammonia etc. [1]. The agriculture and pharmaceutical effluents release pesticides and other chemicals that are responsible for some chronic diseases, harmful for human endocrine, making water not useful for drinking and other uses [2]. There is an urgent need to develop some newer technologies that are eco-friendly in nature and lead to degradation or complete elimination of environmental pollutants and thus prove to be an alternative clean strategy.

Photocatalysis has been attracting attention in recent years due to its potential for green energy and environmental remediation. Studies has been carried out focusing on different types of photocatalysts and different photocatalyst applications [3]. Photocatalysis is inspired by natural photosynthesis [4]. Photosynthesis refers to the process by which green plants, microalgae and some forms of bacteria harvest the energy from the sunlight to power thermodynamically uphill reactions such as the conversion of CO_2 and H_2O to carbohydrate [5]. Photocatalyst is a catalyst that speeds up a chemical reaction using light [6]. The catalyst absorbs the light on surface and creates pairs of electrons and holes that trigger reactions. This process is called photocatalysis. Photocatalysts are used in a variety of applications including sustainable energy production and environmental remediation [7]. Advanced oxidation processes (AOPs) are environmental friendly techniques for the removal of almost all types of pollutants: air pollutants, soil pollutants, water pollutants such as aromatics, petroleum based contents, petroleum hydrocarbons, chlorinated hydrocarbons, pesticides, insecticides, volatile organic compounds (VOC), dyes and other organic materials [8].

2. Basic Principle and Mechanism for Photodegradation

TiO_2 is one of the most widely used photocatalyst to explain photocatalytic process. It relies on the absorption of photons with energy greater than 3.2 eV (corresponding to wavelengths shorter than approximately 390 nm) which triggers an excitation event related to charge separation within the material's bandgap [9]. When wide bandgap semiconductors are irradiated with light of energy higher than their bandgap, electron-hole pairs are generated. This process involves promoting an electron to the conduction band (e_{CB}^-) and creating a positive hole in the valence band (h_{VB}^+).

The h_{VB}^+ and e_{CB}^- act as potent oxidizing and reducing agents respectively. The h_{VB}^+ interacts with organic compounds leading to their oxidation and ultimately producing CO_2 and H_2O as end products. Additionally the h_{VB}^+ can react with water to generate hydroxyl radicals (•OH). Hydroxyl radicals

*Corresponding Author: Shipra Bhardwaj

are highly reactive species with the second-highest oxidation potential (2.80 V) just slightly lower than fluorine, the strongest oxidant known. Due to their electrophilic nature (attraction to electrons) hydroxyl radicals can non-selectively oxidize a wide range of electron-rich organic molecules converting them into CO_2 and water.

$TiO_2 + h\nu$ (<387 nm) $\longrightarrow e_{CB}^- + h_{VB}^+$ .....(32)

$h_{VB}^+ + R \longrightarrow$ intermediates $\longrightarrow CO_2 + H_2O$ ....(33)

$H_2O + h_{VB}^+ \longrightarrow {}^{\bullet}OH + H^{\bullet}$ .....(34)

${}^{\bullet}OH + R \longrightarrow$ intermediates $\longrightarrow CO_2 + H_2O$ ....(35)

where R represents the organic compound. The conductive band can react with O_2 forming an anion radical superoxide as shown in Eq. 36. Further reaction can lead to the formation of hydrogen peroxide which lead to the formation of ${}^{\bullet}OH$. The mechanism of the electron hole-pair formation when the TiO_2 is irradiated, is given in Figure 1.

$e^- + O_2 \longrightarrow O_2^{\bullet -}$ .....(36)

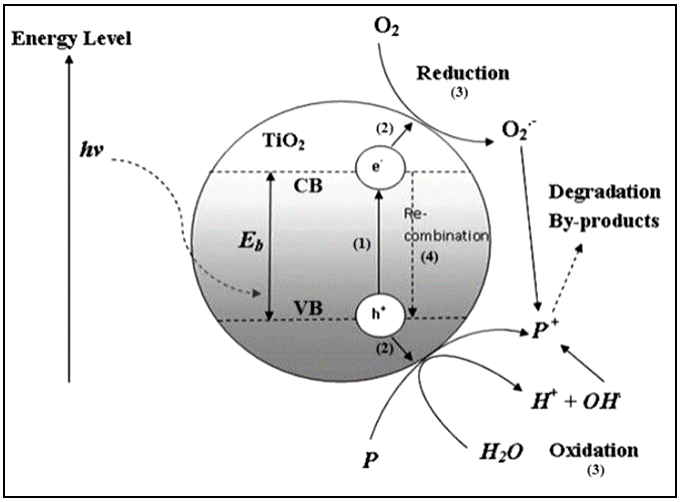

Fig 1: Mechanism of electron-hole pair formation on TiO_2 particle surface

3. Types of Photocatalysis

3.1. Homogeneous Photocatalysis

In homogeneous photocatalysis the reactants and the photocatalysts exist in the same phase. The most commonly used homogeneous photocatalysts include ozone and photo-Fenton systems (Fe^{2+} and Fe^{2+}/H_2O_2). The reactive species is the ${}^{\bullet}OH$ radical which is used for various purposes. The mechanism of hydroxyl radical production by ozone can follow two paths [10].

$O_3 + h\nu \longrightarrow O_2 + O\ (1D)$.....(1)

$O\ (1D) + H_2O \longrightarrow {}^{\bullet}OH + {}^{\bullet}OH$.....(2)

$O\ (1D) + H_2O \longrightarrow H_2O_2$.....(3)

$H_2O_2 + h\nu \longrightarrow {}^{\bullet}OH + {}^{\bullet}OH$.....(4)

Similarly the Fenton system produces hydroxyl radicals by the following mechanism [11]:

$Fe^{2+} + H_2O_2 \rightarrow {}^{\bullet}OH + Fe^{3+} + OH^-$ .....(5)

$Fe^{3+} + H_2O_2 \rightarrow Fe^{2+} + 2{}^{\bullet}OH + H^+$ .....(6)

$Fe^{2+} + {}^{\bullet}OH \rightarrow Fe^{3+} + OH^-$ .....(7)

In photo-Fenton type processes, additional sources of OH radicals should be considered such as photolysis of H_2O_2 and reduction of Fe^{3+} ions under UV light:

$H_2O_2 + h\nu \rightarrow {}^{\bullet}OH + {}^{\bullet}OH$.....(8)

$Fe^{3+} + H_2O + h\nu \rightarrow Fe^{2+} + {}^{\bullet}OH + H^+$.....(9)

The efficiency of Fenton type processes is influenced by several operating parameters like the concentration of hydrogen peroxide, pH, intensity of UV light etc. The main advantage of this process is the ability of using sunlight with light sensitivity up to 450 nm thus avoiding the high costs of UV lamps and electrical energy. These reactions have been proven more efficient than other examples of photocatalysis but the disadvantages of the process are the low pH values, which are required since iron precipitates at higher pH values and the fact that iron has to be removed after treatment.

3.2. Heterogeneous Photocatalysis

Heterogeneous catalysis has the catalysts in a different phase from the reactants. Heterogeneous photocatalysis is a discipline which includes a large variety of reactions: mild or total oxidations, dehydrogenation, hydrogen transfer, $^{18}O_2$–$^{16}O_2$ and deuterium-alkane isotopic exchange, metal deposition, water detoxification, gaseous pollutant removal etc. Most common heterogeneous photocatalysts are transition metal oxides and semiconductors, which have unique characteristics. Unlike metals, which have a continuum of electronic states, semiconductors possess a void energy region where no energy levels are available to promote recombination of an electron and hole produced by photoactivation in the solid. The void region of energy, which extends from the top of the filled valence band to the bottom of the vacant conduction band, is called the band gap [12]. When a photon with energy equal to or greater than the material's band gap is absorbed by the semiconductor, an electron is excited from the valence band to the conduction band, generating a positive hole in the valence band. Such a photogenerated electron-hole pair is termed an exciton. The excited electron and hole can recombine and release the energy gained from the excitation of the electron as heat. Such exciton recombination is undesirable and higher levels lead to an inefficient photocatalyst. For this reason efforts to develop functional photocatalysts often emphasize extending exciton lifetime, improving electron-hole separation using diverse approaches that often rely on structural features such as phase hetero-junctions (e.g. anatase-rutile interfaces), noble-metal nanoparticles, silicon nanowires and substitutional cation doping. The ultimate goal of photocatalyst design is to facilitate reactions of the excited electrons with oxidants to produce reduced products, and/or reactions of the generated holes with reductants to produce oxidized products. Due to the generation of positive holes and excited electrons, oxidation-reduction reactions take place at the surface of semiconductors irradiated with light [13].

In one mechanism of the oxidative reaction, the positive holes react with the moisture present on the surface and produce a hydroxyl radical. The reaction starts by photo-induced exciton generation on the metal oxide surface (MO stands for metal oxide):

$MO + h\nu \rightarrow MO\ (h^+ + e^-)$.....(10)

Oxidative reactions due to photocatalytic effect:

$h^+ + H_2O \rightarrow H^+ + {}^{\bullet}OH$.....(11)

$2h^+ + 2\ H_2O \rightarrow 2H^+ + H_2O_2$.....(12)

$H_2O_2 \rightarrow 2\ {}^{\bullet}OH$.....(13)

Reductive reactions due to photocatalytic effect:

$e^- + O_2 \rightarrow {}^{\bullet}O_2^-$ ……..……(14)

${}^{\bullet}O_2^- + H_2O + H^+ \rightarrow H_2O_2 + O_2$…...……...(15)

$H_2O_2 \rightarrow 2\ {}^{\bullet}OH$……....(16)

Ultimately hydroxyl radicals are generated in both the reactions. These hydroxyl radicals are very oxidative in nature and nonselective with a redox potential of E_0 = +3.06 V [14].

4. Different Types of Photocatalysts Used for Photodegradation

Various types of photocatalysts are known and are being synthesized now a days. Metal based photocatalysts utilizing metals like titanium, zinc, iron etc. are available. Amongst them titanium dioxide (TiO_2) is the most preferred due to its remarkable stability and efficiency [15]. Photocatalysts that are based on semiconductors such as silicon, cadmium sulfide, gallium nitride etc. are also known. These photocatalysts have high electron mobility and can generate highly reactive radicals [16]. Photocatalysts based on carbon materials such as graphene, carbon nanotubes and activated carbon are also prepared and used. These materials have high surface area and can be functionalized to enhance their photocatalytic properties [17]. Photocatalysts that are made by combining two or more different materials are known as composite photocatalysts. For example a composite photocatalyst could be made by combining titanium dioxide with carbon nanotubes to enhance its photocatalytic activity [18].

4.1. Unitary and Binary Photocatalysts Used for Photodegradation

Unitary photocatalysts are materials that are made up of one element and can facilitate chemical reactions using light energy, primarily from photons. These are often oxides, sulfides or other compounds of metals. Titanium dioxide [19] (TiO_2) is widely used due to its chemical stability, non-toxicity and efficiency in generating electron-hole pairs. Unitary photocatalyst materials typically consist of a semiconductor that absorbs light and creates an electron-hole pair which can then interact with a nearby molecule to initiate a chemical reaction. ZnO offers good optoelectronic, catalytic and photochemical properties. Its band gap (3.0 eV) is lower than that of anatase TiO_2, making it a potential alternative for photocatalytic applications. The valence band of ZnO is positioned such that the photogenerated holes stay strong enough to oxidize and decompose many organic compounds due to the position of its valence band [20]. ZnO has been shown to decompose various dyes [21] and environmental pollutants [22]. In some cases, it has outperformed TiO_2 [23] in terms of efficiency. ZnO faces significant limitations like the occurrence of photocorrosion [24] and the susceptibility of ZnO to facile dissolution at extreme pH values that have significantly limited its application in photocatalysis. Kislov *et al* [25] showed that the performance of ZnO can vary significantly depending on the crystallographic orientation.

Cu_2O is a p-type semiconductor and it has a direct band gap of 2.0–2.2 eV which makes it promising for applications in solar energy conversion [26] due to its ability to absorb visible light. The photocatalytic efficiency of Cu_2O is highly influenced by the crystal morphology, as the number of atoms at edges, corners and surfaces varies with shape [27]. Cu_2O octahedra show better photocatalytic activity than cubes because the {1 1 1} facets are more active. This is attributed to the presence of dangling bonds on {1 1 1} surfaces while {1 0 0} facets have saturated bonds and lack dangling bonds [28]. Zhang *et al* [27] synthesized mixed 26-facet and 18-facet polyhedron using a hydrothermal process with stearic acid as a structure-directing agent. These polyhedrons displayed higher photocatalytic activity in the decomposition of methyl orange (MO) compared to Cu_2O octahedron and cubes. Huang *et al* [29] tested Cu_2O nanoparticles and microparticles for the photodegradation of methyl orange, demonstrating their potential in environmental remediation.

WO_3 (tungsten trioxide) is a visible light-responsive photocatalyst. WO_3 can absorb light up to 480 nm, making it responsive to the visible light spectrum. This feature makes it valuable for solar-driven photocatalysis. WO_3 often exhibits low photoactivity due to high recombination rate of photogenerated electron-hole pairs despite its visible light absorption capabilities, which reduces the efficiency of photocatalytic reactions and low electron transfer rate to oxygen [30] (O_2), limiting the formation of reactive oxygen species needed for pollutant degradation. A study comparing WO_3, TiO_2, NiO and Fe_2O_3 for phenol degradation in water under 355 nm pulsed laser irradiation showed that WO_3 [31] achieved the highest degradation. This was attributed to WO_3's band gap which allows it to efficiently absorb energy under laser irradiation. Under laser illumination, WO_3 showed enhanced activity for phenol degradation. Films anodically grown on tungsten foil substrates demonstrated photoactivity under visible light. These films were effective in oxidation of methylene blue and reductive conversion of Cr (VI) [32], highlighting WO_3's dual functionality in both oxidation and reduction reactions. WO_3's visible light activity offers promise for environmental applications, though improving electron-hole separation remains a key challenge.

Single-crystalline V_2O_5 nanowires were grown on sapphire and ITO-coated glass substrates via the thermal decomposition of a precursor film, which was spin-coated from an organic vanadium solution [33]. This method enables precise control over the nanowire growth and orientation. These nanowires were shown to be more efficient than bulk V_2O_5 for the degradation of Toluidine Blue O dye under ultraviolet (UV) irradiation. The high surface area-to-volume ratio of the nanowires enhances their interaction with the dye molecules and increases the availability of active sites for photocatalysis. The nanowires were found approximately 5 µm in length with an average diameter of 100 nm, providing a well-defined structure that is advantageous for photocatalytic reactions.

Iron(III) hydroxides can absorb light up to 600 nm which makes them suitable for visible light photocatalysis. However they typically suffer from rapid electron-hole recombination [34] which reduces their overall photocatalytic efficiency. Mazellier and Bolte [35] synthesized goethite (α-FeOOH) which was tested for the photodegradation of 2,6-dimethylphenol. Goethite is one of the commonly studied iron oxides for environmental remediation. Bandara *et al* [36] investigated the photocatalytic degradation of various chlorophenols using aqueous suspensions of α-Fe_2O_3 and α-FeOOH under simulated solar radiation. Both materials showed promise in breaking down chlorophenols which are common environmental pollutants. Wang *et al* [37] explored four different iron oxides for the photodegradation of pyrene under UV irradiation. This study demonstrates the versatility of iron oxides for degrading different organic pollutants. Anodic-biased α-Fe_2O_3 films, formed through metal organic deposition, exhibited high photocatalytic activity for the decomposition of 2-naphthol under visible light irradiation [38]. The anodic bias likely helped suppress electron-hole recombination, enhancing performance. Li *et al* [39]

synthesized Fe_2O_3 hollow spheres with mesopores using a hydrothermal process without templates. These hollow spheres outperformed ring-like α-Fe_2O_3 nanoparticles for the photodegradation of salicylic acid, likely due to their large surface area and efficient light absorption. Hollow microspheres made of α-Fe_2O_3 nanorods were found to be effective photocatalysts for the direct degradation of methyl orange [40], a common dye pollutant. The nanorod structure of the microspheres enhances their photocatalytic properties.

Cadmium sulfide (CdS) is a widely researched photocatalyst due to its direct band-gap energy of 2.42 eV, which enables it to effectively utilize visible light. CdS has been extensively studied for hydrogen production from water via photocatalysis under visible light and photovoltaic devices where its ability to absorb visible light makes it useful in solar cells. CdS is unsuitable for the photocatalytic removal of organic pollutants because of its susceptibility to Photocorrosion [41] and release of toxic cadmium ions. Yang *et al* [42] developed a more stable and regenerable CdS photocatalyst by incorporating CdS nanoparticles into hexagonal mesoporous silica spheres and coating them with a polyelectrolyte layer. This method provided two major benefits such as increased stability and reusability. The coated CdS catalyst remained active for over 22 cycles of photocatalysis, degrading dyes and phenolic compounds without any leakage of cadmium into the solution. In contrast uncoated CdS lost activity after just three cycles, making the coating highly effective.

4.2. Ternary Photocatalyst Used for Photodegradation

A ternary photocatalyst involves three different components which are combined to optimize photocatalytic performance. The three components can offer multiple synergistic effects such as enhanced light absorption, improved charge separation and catalytic activity. Bismuth vanadate ($BiVO_4$) has garnered significant attention as a photocatalyst for oxygen (O_2) evolution under visible light [43] due to its promising photoactivity. $BiVO_4$ exists in three crystalline forms monoclinic scheelite-type, tetragonal scheelite-type and tetragonal zircon-type. Among these only the monoclinic phase exhibits strong photocatalytic properties under visible light irradiation [44]. Kohtani *et al* [45] reported that $BiVO_4$ can efficiently degrade long-chain alkylphenols and polycyclic aromatic hydrocarbons (PAHs) under visible light, demonstrating its potential for environmental remediation. A highly efficient monoclinic $BiVO_4$ photocatalyst was synthesized using an aqueous method assisted by cetyltrimethylammonium bromide [46] (CTAB). The photocatalytic activity was tested through the degradation of rhodamine B (RhB) under visible light and the as-prepared a reference $BiVO_4$ prepared by a similar aqueous method and $BiVO_4$ prepared via a solid-state reaction. The superior photocatalytic activity of this $BiVO_4$ sample was attributed to the presence of an impurity level in the band gap, which enhances its ability to absorb visible light and reduces electron-hole recombination

Silver vanadate (Ag_3VO_4) powders synthesized by precipitation [47] have shown remarkable photocatalytic performance, especially under visible light irradiation. Ag_3VO_4 powders were evaluated for the decolorization of acid red B, a common dye pollutant, under visible light. All Ag_3VO_4 samples significantly outperformed TiO_2, which is often the benchmark for photocatalytic materials. The samples prepared with an excess of vanadium or silver showed higher photocatalytic activity than those prepared with a stoichiometric ratio of Ag_3VO_4. This indicates that slight compositional variations can enhance the photocatalytic performance, potentially by modifying the band structure or surface properties. The photocatalytic activity of Ag_3VO_4 was further increased by 3.8 times when NiO was loaded on the surface of Ag_3VO_4. The presence of NiO improved charge separation by acting as a co-catalyst, reducing electron-hole recombination and enhancing the overall efficiency of the system.

Indium vanadate ($InVO_4$) is a visible light-responsive photocatalyst [48] with a band gap of approximately 2.0 eV, offering potential for a variety of applications under solar irradiation. $InVO_4$ is typically prepared using solid-state or melting reactions, which is non-homogeneous materials, low surface area and limiting the availability of active sites for photocatalysis. Zhang *et al* [49] addressed these limitations by preparing $InVO_4$ nanoparticles through the calcination of an amorphous complex precursor at a relatively low temperature of 600°C. The photocatalytic activity of the synthesized $InVO_4$ nanoparticles was tested for the decomposition of gaseous formaldehyde under both UV and visible light irradiation.

Nanosized $CeVO_4$, $PrVO_4$ and $NdVO_4$ were synthesized under microwave assisted radiations and their photocatalytic activity was investigated by degrading various dyes and some phenols [50]. It offered several advantages over traditional solid-state synthesis such as faster reaction times, better homogeneity of the resulting materials and improved crystallinity and nanoscale control. The degradation rates of these pollutants in the presence of the microwave-synthesized materials were significantly higher than those of samples prepared by solid-state techniques and P25 TiO_2 which is often used as a reference photocatalyst in such studies.

Bismuth tungstate (Bi_2WO_6), one of the simplest aurivillius oxides, has a layered structure comprising WO_6 perovskite-like slabs and shows excellent photocatalytic properties under visible light irradiation due to its band gap of 2.7–2.8 eV. Tang *et al* [51] first demonstrated that Bi_2WO_6 is effective for photocatalytic oxygen (O_2) evolution, mineralization of pollutants such as chloroform ($CHCl_3$) and acetaldehyde (CH_3CHO), indicating its potential for the degradation of organic contaminants. Amano *et al* [52] found that the photocatalytic performance of Bi_2WO_6 is highly dependent on its crystallinity. Hydrothermally synthesized Bi_2WO_6 crystallites were capable of inducing the complete oxidative decomposition of gaseous acetaldehyde even under visible light irradiation. In contrast amorphous Bi_2WO_6 showed negligible photoactivity due to rapid electron-hole recombination which limits its effectiveness. Bi_2WO_6 was found to be effective for the photocatalytic inactivation of E. coli, demonstrating its potential for microbial disinfection [53]. It was also used to effectively eliminate marine microalgae such as amphidinium carterae and tetraselmis suecica, showing promise for water treatment applications [54].

Bi_2MoO_6 shares similar crystalline patterns with Bi_2WO_6, making it another aurivillius-type oxide with excellent visible light-responsive photocatalytic properties [55]. Bi *et al* [56] synthesized Bi_2MoO_6 outperformed the well-known photocatalyst Degussa P25 in the decomposition of rhodamine B (RhB). Hydrothermal method of preparation exhibited excellent photocatalytic efficiency for the degradation of both RhB and methylene blue (MB) [57]. Nanocrystals prepared by this method exhibited 4–6 times higher photocatalytic activity compared to those produced via traditional solid-state reactions, underscoring the importance

of synthesis techniques in optimizing photocatalytic performance [58]. γ-Bi_2MoO was investigated for RhB degradation under visible light with various morphologies and surface structures [59].

Zinc tungstate ($ZnWO_4$) had been extensively studied as a potential photocatalyst, particularly for environmental applications such as pollutant degradation [60]. $ZnWO_4$ and Bi_2WO_6 were both tested for the photocatalytic degradation of rhodamine B (RhB) under UV illumination and both exhibited high activity [61]. Bi_2WO_6 demonstrated excellent photocatalytic performance across a wider spectrum, including the visible light region. $ZnWO_4$ was primarily active in the UV region, limiting its application under natural sunlight. The photocatalytic performance of $ZnWO_4$ was found to depend on the hydrothermal crystallization processes produced highly active $ZnWO_4$ [62] and $ZnWO_4$ synthesized by calcining a co-precipitated precursor also demonstrated high photocatalytic activity for the degradation of gaseous formaldehyde, outperforming the widely-used P25 TiO_2 [63]. Porous $ZnWO_4$ films prepared on ITO glass, using an amorphous heteronuclear complex and polyethylene glycol (PEG), have demonstrated outstanding photocurrent response and high photocatalytic activity [64].

4.3. Quaternary Photocatalyst Used for Photodegradation

Single-phase quaternary oxide materials had been studied with the aim to develop novel photocatalysts showing high activity in the visible light region. Luan and collaborators [65-67] synthesized Bi_2MTaO_7 (where M = Ga, In, La, Y), were tested for their ability to degrade methyl blue (MB) and rhodamine B (RhB) under visible light. The solid-state reactions among single-metal oxides allowed for tuning of the band gap in these multiple-metal oxides. Compounds such as M_2BiNbO_7 [68] (where M = In and Ga) were also investigated. These niobium-containing oxides showed promising photocatalytic performance under visible light. Bi_2MVO_7 [69-72] (where M = Ga, Fe, Al, Sb) were tested for their efficiency in degrading MB and RhB. Y_2MSbO_7 [73,74](where M = Fe, In) were examined and showed activity under visible light. Quaternary oxides such as Ga_2BiTaO_7 [75], Gd_2YSbO_7 [76], Gd_2BiSbO_7 [76] and Bi_2YVO_8 [77] were also found to be active under visible light.

Nb-containing oxides such as $CsBiNb_2O_7$, $CsBi_2Nb_5O_{16}$ and $PbBi_2Nb_2O_9$, were explored for their effectiveness in the visible light-driven decomposition of gaseous 2-propanol. $CsBi_2Nb_5O_{16}$ demonstrated superior photocatalytic activity compared to $CsBiNb_2O_7$ [78]. $PbBi_2Nb_2O_9$ [79] (with a band gap of 2.88 eV) outperformed TiO_2 − xNx (with a band gap of 2.73 eV). The higher activity of $RbBi_2Nb_5O_{16}$ is related to its distinct absorption properties, which enhance its ability to degrade gaseous acetaldehyde under visible light. $RbBiNb_2O_7$ also showed photocatalytic activity but it was found less effective than $RbBi_2Nb_5O_{16}$ [80].

$LiBi_4Ta_3O_{14}$ [81] had a band gap of 3.5 eV while $LiBi_4Nb_3O_{14}$ had a lower band gap of 3.0 eV. $LiBi_4Nb_3O_{14}$ demonstrated higher efficiency in degrading phenolic compounds compared to $LiBi_4Ta_3O_{14}$. Both materials had relatively low surface areas which could limit their photocatalytic efficiency. Despite this, their band gap and chemical properties enabled reasonable photocatalytic activity. Ba_2RBiO_6 (R = La, Ce, Nd, Sm, Eu, Gd, Dy) samples with a double-perovskite structure showed very high activities for the degradation of MB and gaseous 2-propanol under visible light illumination [82].

Garza-Tovar *et al* [83] developed a sol–gel route for preparing Bi_2MNbO_7 (M = Al, In, Fe, Sm) using metalorganic precursors. This method involved a sol–gel process followed by annealing at 400 °C. The sol–gel synthesized materials demonstrated superior photocatalytic activity for methylene blue (MB) degradation under UV illumination compared to those prepared by solid-state reactions or the standard P25 photocatalyst. Bi_2InTaO_7 [84] prepared via the sol–gel method, exhibited high efficiency in the UV-induced degradation of alizarin red S.

Li *et al* [85] utilized a cation exchange method to synthesize polycrystalline Ag_2ZnGeO_4. The process involved using Na_2ZnGeO_4 as the parent compound and was conducted at a relatively low temperature of 220 °C. The Ag_2ZnGeO_4 sample showed good activity for the photodegradation of RhB and Orange II. RhB was completely degraded and 69.2% of Orange II was converted after 360 min of visible light (> 420 nm) irradiation.

Lin *et al* [86-88] investigated these materials for the degradation of methyl orange (MO) and other pollutants under UV and visible light irradiation. Bi_4NbO_8Cl demonstrated exceptional efficiency for visible light photocatalysis. It outperformed the ternary oxychloride Bi_3O_4Cl (band gap = 2.80 eV) and anatase TiO_2. Photoactivity order is Bi_4NbO_8Cl > Bi_3O_4Cl > anatase TiO_2. $Na_{0.5}Bi_{1.5}O_2Cl$ had band gap = 3.44 eV under visible light. The photoactivity followed the order $Na_{0.5}Bi_{1.5}O_2Cl$ > TiO_2 > BiOCl. $PbBiO_2Br$ showed higher photocatalytic activity compared to $PbBi_2Nb_2O_9$, TiO_2 −xNx and BiOBr under visible light. Photoactivity order is Bi_3O_4Cl> anatase TiO_2 >Bi_4NbO_8Cl. $Na_{0.5}Bi_{1.5}O_2Cl$ is less active under UV light compared to BiOCl. Photoactivity order is BiOCl > $Na_{0.5}Bi_{1.5}O_2Cl$ > TiO_2.

5. Factors Affecting the Performance of Photocatalysts

Several factors affect the performances of photocatalysts. Considering the removal of colored pollutants, factors that affect the performance of photocatalysts like concentration of dyes, pH of the solution, catalyst dosage, intensity of light, intermediate species etc. are considered and discussed here by.

Initial concentration of dyes significantly affects the performance of photocatalytic degradation. Different dyes have varying functional groups that influence how they interact with photocatalysts. This means the optimal dye concentration depends on the dye's nature. Higher concentrations typically accelerate reactions. Degradation performance of Photocatalyst decreases with higher dye concentrations due to reduced ratio of active photocatalyst sites to dye molecules, fewer OH radicals available per dye molecule and light absorption by the dye, limiting light penetration to the catalyst surface. Degradation dropped from 77% to 42% as dye concentration increased from 100 to 400 mg/L [89]. Degradation rates of 72%, 85%, and 93% were achieved at initial dye concentrations of 0.0063, 0.015 and 0.0188M [90]. Degradation decreased from 80% to 19% with initial dye concentrations increasing from 50 to 200 mg/L [91]. Degradation improved from 39% to 65% as initial dye concentration decreased from 300 to 100 mg/L [92].

The pH significantly affects the electrostatic interactions between the photocatalyst, dye molecules, and reactive oxygen species (ROS), influencing the degradation process. Umar and Halim [93] observed that the highest photocatalytic oxidation performance of TiO_2 occurred at pH 2. For rhodamine B and methylene blue, photodegradation was higher at an alkaline pH (pH 10) [94]. Bismuth ferrite catalysts demonstrated the highest rhodamine B degradation at neutral

pH [95]. ZnO–rGO catalysts also achieved optimal methylene blue degradation at neutral pH [96].

Photodegradation efficiency generally increases with an increase in catalyst dose [97] because more electron-hole pairs are generated, enhancing the reaction rate. Beyond a certain catalyst dose, the mixture becomes more turbid, reducing light penetration to the catalyst surface and leading to a decrease in the reaction rate. Lu *et al* [98] found that increasing the CdS/graphene catalyst dose initially improved the photodegradation of rhodamine B (49% to 86%) as the dose increased from 200 to 1800 mg/L, but further increases in the dose reduced efficiency.

The adsorption of dyes on the surface of photocatalysts plays a crucial role in determining the efficiency of photocatalytic degradation. This process is influenced by the binding affinities and electrostatic interactions between dye molecules and the catalyst surface. Strong Adsorption causes catalyst poisoning by overly covering the surface, blocking photon access and reducing photocatalytic performance. Weak Adsorption does not allow proper attachment of dye molecules, leading to ineffective degradation. Moderate adsorption as per the Sabatier principle, optimal photocatalytic performance is achieved with moderate adsorption, which balances photocatalysis and adsorption for better dye degradation [99].

The efficiency of photocatalytic degradation of dyes largely depends on the energy provided by light irradiation, which generates positive holes and electrons in the valence and conduction bands of photocatalysts. The energy of the light must meet or exceed the photocatalyst band gap energy for these charge carriers to form. Higher light intensity increases photocatalytic performance by boosting the penetration of light and enhancing charge carrier generation. For instance, studies have shown that increasing light intensity from 16W to 62W resulted in a 33% higher degradation of reactive yellow dye [100]. Similarly, the effect of light intensity on other dyes like fast green has also demonstrated enhanced degradation with increased light intensity.

6. Applications of Photocatalysts

Photocatalytic decolorization of dyes using AOP is a recent concern among researchers since it offers an attractive method for decolorization of dyes and breaks them into simple mineral form. Kumar and Ameta [101] studied the photodegradation of basic orange 12 using the H_2O_2/Fe^{3+} system, demonstrating the effectiveness of the photo-Fenton process in breaking down complex dye molecules. Kusic *et al* [102] compared the degradation kinetics of reactive blue 49 and reactive blue 137 using various dark- and photo-Fenton systems. The UV/Fe^{2+}/H_2O_2 system showed superior degradation rates due to enhanced radical generation under UV light. Garcia-Montano *et al* [103] conducted solar-assisted photo-Fenton degradation of procion red H-E7B, tracking heteroatom oxidation products like NH_4^+, NO_3^-, Cl^-, and short-chain carboxylic acids. This study highlights the environmental benefits of mineralizing dyes into non-toxic compounds. Zheng *et al* [104] demonstrated the efficiency of the Fenton and photo-Fenton processes in degrading eosin Y and showed that oxalic acid can significantly enhance photocatalytic efficiency in solar-driven systems. Sun *et al* [105] investigated the spectral changes of amido black 10B during Fenton treatment, showing that the azo linkage in the dye was more readily broken down than the aromatic rings. This study emphasizes the importance of dye structure on the degradation efficiency. Daneshvar and Khataee [106] studied the removal of acid red 14 using different Fenton-based processes. They reported that the UV/H_2O_2/Fe(III)/oxalate system had the highest decolorization efficiency within 2 minutes. The presence of oxalate was crucial in enhancing Fe(III) photoreduction under UV light. Zheng and Xiang [107] investigated the photo-Fenton degradation of rhodamine B, revealing that both the dye and its chemical oxygen demand (COD) could be effectively removed. This study underscores the dual role of AOPs in decolorization and mineralization. Neamtu *et al* [108] examined the degradation of reactive yellow 84 and reactive red 120 using various Fenton-like systems. Solar-driven Fe^{2+}/H_2O_2 showed the fastest degradation rates, followed by UV-assisted systems. This emphasizes the importance of light sources in enhancing dye removal efficiency. Xie *et al* [109] studied the photo-Fenton degradation of acridine orange and alizarin violet 3B under visible light, identifying intermediates like N,N-dimethyl formaldehyde and N,N-dimethyl acetamide. This study illustrates the complex breakdown pathways of dyes during photocatalysis. Wu *et al* [110] explored the degradation of malachite green under visible light in the presence of Fe^{3+}/H_2O_2 and Fe^{2+}/H_2O_2. They proposed a mechanism involving electron transfer from the excited dye molecules to Fe^{3+}, highlighting the role of dye excitation in enhancing degradation efficiency.

Alalm *et al* [111] investigated the degradation of chlorpyrifos, lambda-cyhalothrin, and diazinon from real industrial wastewater using solar photo-Fenton and solar TiO_2 photocatalysis. These processes demonstrated efficient removal of these pesticide contaminants, offering a sustainable approach to wastewater treatment. Dbira *et al* [112] studied the photo-Fenton degradation of *2*-chloro-4,6-diamino-1,3,5-triazine in aqueous solutions. Total organic carbon (TOC) and total Kjeldahl nitrogen (TKN) analyses indicated that carbon dioxide (CO_2) and ammonia (NH_3) were not produced during treatment, suggesting that the triazine ring remained largely intact, with only substituent groups being released. Sanchez *et al* [113] conducted an economic evaluation of a combined photo-Fenton and membrane bioreactor (MBR) process for treating pesticide-contaminated wastewater. This hybrid approach highlights the cost-effectiveness and efficiency of integrating AOPs with biological treatments. Vilar *et al* [114] investigated the improvement of biodegradability in wastewater containing pesticides from phytopharmaceutical plastic containers. A solar photo-Fenton step was used prior to biological oxidation, showing significant enhancement in biodegradability, which is crucial for subsequent biological treatment processes. Karci *et al* [115] examined the transformation of 2,4-dichlorophenol by H_2O_2/UV-C, Fenton, and photo-Fenton oxidation. Farree *et al* [116] studied the degradation of biorecalcitrant pesticides such as alachlor, atrazine, chlorfenvinphos, diuron, isoproturon, and pentachlorophenol using a combination of homogeneous photo-Fenton/ozone (PhFO) and heterogeneous TiO_2-photocatalysis/ozone (PhCO) systems. These combined methods were highly effective in breaking down stubborn pesticide molecules into less harmful substances. Derbalah *et al* [117] investigated the photocatalytic removal kinetics of fenitrothion at a concentration of 0.5 mg/L in both pure and natural waters using Fe^{3+}/H_2O_2/UV-Vis, Fe^{3+}/UV-Vis, and H_2O_2/UV-Vis oxidation systems.

Orbeci *et al* [118] evaluated a modified photo-Fenton procedure designed for degrading antibiotics in aqueous solutions. A photocatalytic reactor with continuous recirculation was equipped with a high-pressure mercury lamp surrounded by

iron mesh. The study showed that this modified procedure improves the efficiency of antibiotic degradation, offering a sustainable solution for treating contaminated water. Batista and Nogueira [119] focused on the photo-Fenton degradation of sulfonamide antibiotics, sulfadiazine and sulfathiazole, mediated by Fe^{3+}-oxalate. This study highlights the importance of iron-complex-mediated reactions in enhancing photocatalytic degradation in aqueous solutions. Pérez-Moya *et al* [120] characterized the photo-Fenton degradation of the antibiotic sulfamethazine. Their results emphasize the identification of degradation intermediates, which is crucial for understanding the complete mineralization pathway of antibiotics during treatment. Radjenović *et al* [121] investigated the solar photocatalytic degradation of ranitidine using TiO_2 and Fenton reagent (Fe^{2+}/H_2O_2) at a pilot scale. The characterization of intermediate products was also studied, offering insight into real-world applications for pharmaceutical wastewater treatment. Giri and Golder [122] conducted a comparative study on the degradation of 4-methylaminoantipyrine (4-MAA), a hydrolysis product of the analgesic dipyrone. Karale *et al* [123] investigated the degradation of 3-aminopyridine (3AP), a plant growth regulator and emerging pollutant. Both Fenton and photo-Fenton oxidation were evaluated under different conditions (pH, hydrogen peroxide, and iron salts). Alalm *et al* [124] investigated the solar photo-Fenton degradation of four pharmaceuticals: amoxicillin, ampicillin, diclofenac, and paracetamol. Elmolla and Chaudhuri [125] evaluated the photo-Fenton treatment of wastewater containing amoxicillin and cloxacillin. Baydum *et al* [126] studied the degradation of propranolol using different oxidation processes (UV-C direct photolysis, H_2O_2, UV-C/H_2O_2, UV-C/Fe^{2+}, H_2O_2/Fe^{2+}, and UV-C/H_2O_2/Fe^{2+}). Sirtori *et al* [127] investigated the treatment of pharmaceutical wastewater containing high levels of nalidixic acid (45 mg/L) using a solar photo-Fenton/biological process. The study demonstrated that combining AOPs (solar photo-Fenton) with biological treatment improved overall degradation efficiency (>95%).

Conclusion

In conclusion, photocatalysis has shown great promise in addressing environmental challenges such as water, air purification and in the production of renewable fuels through processes like water splitting and CO_2 reduction. The field of photocatalysis and photochemistry has seen many improvements. It has driven by the need for sustainable and efficient energy solutions. Through this comprehensive review we have highlighted different types of photocatalysts, their properties and their applications in environmental remediation. Titanium dioxide (TiO_2) remains the most extensively studied photocatalyst due to its stability, non-toxicity and cost-effectiveness. However limitations such as its wide bandgap necessitate the exploration of alternative materials and doping strategies to enhance visible light absorption limits its use as photocatalyst. Efforts to improve the efficiency of photocatalytic processes have focused on several strategies including the design of heterojunctions, surface modifications and the incorporation of co-catalysts. These approaches aim to reduce recombination rates of electron-hole pairs and enhance light harvesting. Photocatalysis has shown great promise in addressing environmental challenges such as water, air purification and in the production of renewable fuels through processes like water splitting and CO_2 reduction. Future research is likely to focus on the development of multi-functional photocatalysts, the integration of photocatalytic systems with other renewable energy technologies and the exploration of bio-inspired and hybrid materials.

References

1. Mutamim NSA, Noor ZZ, Hassan MAA, Olsson G. Application of membrane bioreactor technology in treating high strength industrial wastewater: a performance review. *Desalination*, 2011, 305, 1-11.
2. Das R. Application photocatalysis for treatment of industrial waste water: a short review. *Open Acc. Lib. J.,* 2014; 1:1-17.
3. Low XJ, Yu GJ, Jaroniec M, Wageh S and Al-Ghamdi AA. *Adv. Mater,* 2017; 29:1601694.
4. Golbeck JH, Ed.; *Springer*: Dordrecht, the Netherlands, 2006, 205−222.
5. Larkum, Curr. Opin. *Biotechnol*, 2010, 21, 271.
6. Wu J, Zheng W & Chen Y. Definition of photocatalysis: Current understanding and perspectives. *Curr. Opinion Green Sust. Chem.* 2022; 33:100580.
7. Garg A, Basu S, Shetti NP & Reddy KR. 2D materials and its hetero structured photocatalysts: Synthesis, properties, functionalization and applications in environmental remediation. *J Environ. Chem. Eng.*, 2021; 9(6):106408.
8. Zhang T, Wang X, Zhang X. Recent progress in TiO_2-mediated solar photocatalysis for industrial wastewater treatment. *Int. J. Photoenergy*, 2014; 12:607954.
9. Boroski M, Rodrigues AC, Garcia JC, Sampaio LS, Nozaki J, Hioka N. Combined Electrocoagulation and TiO_2 Photoassisted Treatment Applied to Wastewater Effluents from Pharmaceutical and Cosmetic Industries. *Journal of Hazardous Materials*, 2009; (162):448–454.
10. Wu CH, & Chang CL. Decolorization of Reactive Red 2 by advanced oxidation processes: Comparative studies of homogeneous and heterogeneous systems. *Journal of hazardous material.* 2006; 128(2-3):265-272.
11. Peternel IT, Koprivanac N, Bozic AM, Kusic HM. Comparative study of UV/TiO_2, UV/ZnO and photo-Fenton processes for the organic reactive dye degradation in aqueous solution. *Journal of Hazardous Materials,* 2007; 148(1–2):477–84.
12. Schlogl R. Heterogeneous catalysis. *Angewandte Chemie International Edition*, 2015; 54(11):3465-3520.
13. Ibhadon AO & Fitzpatrick P. Heterogeneous photocatalysis: recent advances and applications. *Catalysts,* 2013; 3(1):189–218.
14. Swift E. A durable semiconductor photocatalyst. *Science*, 2019; 365(6451):320-321.
15. Fujishima A, Rao TN, Tryk DA. Titanium Dioxide Photocatalysis. *Journal of Photo- chemistry and Photobiology C Photochemistry Reviews*, 2000; 1:1-21
16. Vaya D & Surolia PK. Semiconductor based photocatalytic degradation of pesticides: An overview. Environ. Tech. & Innov., 2020; 20:101128.
17. Li Z, Li K, Du P, Mehmandoust M, Karimi F & Erk N. Carbon-based photocatalysts for hydrogen production: A review. *Chemosphere*, 2022, 135998.
18. Humayun M, Wang C & Luo W. Recent progress in the synthesis and applications of composite photocatalysts: a critical review. *Small Methods*. 2022; 6(2):2101395.
19. Fujishima A. Electrochemical photolysis of water at a semiconductor electrode. *Nature*, 1972; 238:38–40.
20. Miyauchi M, Nakajima A, Watanabe T, Hashimoto K. Photocatalysis and photoinduced hydrophilicity of

various metal oxide thin films. *Chem. Mater.,* 2002*;* 14:2812–2816.
21. Akyol A, Bayramoglu M. Photocatalytic degradation of Remazol Red F3B using ZnO catalyst. *J. Hazard. Mater.*, 2005; 124:241–246.
22. Kandavelu V, Kastien H, Thampi RK. Photocatalytic degradation of isothiazolin-3-ones in water and emulsion paints containing nanocrystalline TiO_2 and ZnO catalysts. *Appl. Catal. B: Environ.* 2004; 48:101–111.
23. Chen CC. Degradation pathways of ethyl violet by photocatalytic reaction with ZnO dispersions. *J. Mol. Catal. A: Chem.* 2006; 264:82–92.
24. Domenech J, Prieto A. Stability of ZnO particles in aqueous suspensions under UV illumination. *J. Phys. Chem.* 1986; 90:1123–1126.
25. Kislov N, Lahiri J, Verma H, Goswami YD, Stefanakos E, Batzill M. Photocatalytic degradation of methyl orange over single crystalline ZnO: orientation dependence of photoactivity and photostability of ZnO. *Langmuir*, 2009; 25:3310–3315.
26. Hara M, Kondo T, Komoda M, Ikeda S, Shinohara K, Tanaka A, Kondo NJ, Domen K. Cu_2O as a photocatalyst for overall water splitting under visible light irradiation. *Chem. Commun.,* 1998, 357–358.
27. Zhang Y, Deng B, Zhang T, Gao D, Xu WA. Shape effects of Cu_2O polyhedral microcrystals on photocatalytic activity. *J Phys. Chem. C,* 2010; 114:5073–5079.
28. Xu H, Wang W, Zhu W. Shape evolution and size-controllable synthesis of Cu_2O octahedra and their morphology-dependent photocatalytic properties. *J. Phys. Chem. B*, 2006; 110:13829–13834.
29. Huang L, Peng F, Yu H, Wang H. Preparation of cuprous oxides with different sizes and their behaviours of adsorption, visible-light driven photocatalysis and photocorrosion. *Solid State Sci.*, 2009; 11:129–138.
30. Sclafani A, Palmisano L, Marcì G, Venezia MA. Influence of platinum on catalytic activity of polycrystalline WO_3 employed for phenol photodegradation in aqueous suspension. *Sol. Energy Mater. Sol. Cells.* 1998; 51:203–219.
31. Gondal AM, Sayeed NM, Alarfaj A. Activity comparison of Fe_2O_3, NiO, WO_3, TiO2 semiconductor catalysts in phenol degradation by laser enhanced photocatalytic process. *Chem. Phys. Lett.*, 2007; 445:325–330.
32. Watcharenwong A, Chanmanee W, Tacconi RN, Chenthamarakshan RC, Kajitvichyanukul P, Rajeshwar K. Anodic growth of nanoporous WO_3 films: morphology, photoelectrochemical response and photocatalytic activity for methylene blue and hexavalent chrome conversion. *J. Electroanal. Chem.*, 2008; 612:112–120.
33. Shahid M, Rhen SD, Shakir I, Patole PS, Yoo BJ, Yang JS, Kang JD. Facile synthesis of single crystalline vanadium pentoxide nanowires and their photocatalytic behavior. *Mater. Lett.*, 2010; 64:2458–2461.
34. Leland KJ, Bard JA. Photochemistry of colloidal semiconducting iron oxide polymorphs. *J. Phys. Chem.*, 1987; 91:5076–5083.
35. Mazellier P, Bolte M. Heterogeneous light-induced transformation of 2, 6- dimethylphenol in aqueous suspensions containing goethite. *J. Photochem. Photobiol. A: Chem.*, 2000; 132:129–133.
36. Bandara J, Mielczarski AJ, Lopez A, Kiwi J. Sensitized degradation of chlorophenols on iron oxides induced by visible light. Comparison with titanium oxide. *Appl. Catal. B: Environ.*, 2001; 34:321–333.
37. Wang Y, Liu SC, Li BF, Liu PC, Liang BJ. Photodegradation of polycyclic aromatic hydrocarbon pyrene by iron oxide in solid phase. *J. Hazard. Mater.*, 2009; 162:716–723.
38. Kawahara T, Yamada K, Tada H. Visible light photocatalytic decomposition of 2-naphthol by anodic-biased α -Fe_2O_3 film. *J. Colloid Interface Sci.*, 2006; 294:504-507.
39. Li L, Chu Y, Liu Y, Dong L. Template-free synthesis and photocatalytic properties of novel Fe_2O_3 hollow spheres. *J. Phys. Chem.*, 2007; 111:2123–2127.
40. Xie X, Yang H, Zhang F, Li L, Ma J, Jiao H, Zhang J. Synthesis of hollow microspheres constructed with α-Fe_2O_3 nanorods and their photocatalytic and magnetic properties. *J. Alloys Compd.*, 2009; 477:90–99.
41. Meissner D, Memming R, Kastening B. Photoelectro-chemistry of cadmium sulfide. 1. Reanalysis of photo-corrosion and flat-band potential. *J Phys. Chem.* 1988; 92:3476–3483.
42. Yang Y, Ren N, Zhang Y, Tang Y. Nanosized cadmium sulfide in polyelectrolyte protected mesoporous sphere: a stable and regeneratable photocatalyst for visible-light-induced removal of organic pollutants. *J. Photochem. Photobiol. A: Chem.* 2009; 201:111–120.
43. Kudo A, Omori K, Kato H. A novel aqueous process for preparation of crystal form-controlled and highly crystalline $BiVO_4$ powder from layered vanadates at room temperature and its photocatalytic and photophysical properties. *J. Am. Chem. Soc.*, 1999; 121:11459–11467.
44. Yu QJ, Kudo A. Effects of structural variation on the photocatalytic perfor mance of hydrothermally synthesized $BiVO_4$. *Adv. Funct. Mater.*, 2006; 16:2163–2169.
45. Kohtani S, Makino S, Kudo A, Tokumura K, Ishigaki Y., Matsunaga T, Nikaido O, Hayakawa K, Nakagaki R. Photocatalytic degradation of 4-nonylphenol under irradiation from solar simulator: comparison between $BiVO_4$ and TiO_2 photocatalysts. *Chem. Lett.*, 2002; 31:660–661.
46. Yin W, Wang W, Zhou L, Sun S, Zhang L. CTAB-assisted synthesis of mono clinic $BiVO_4$ photocatalyst and its highly efficient degradation of organic dye under visible-light irradiation. *J Hazard. Mater.*, 2010; 173:194–199.
47. Hu X, Hu C. Preparation and visible-light photocatalytic activity of Ag_3VO_4 powders. *J. Solid State Chem.* 2007; 180:725–732.
48. Ye J, Zou Z, Oshikiri M, Matsushita A, Shimoda M, Imai M, Shishido T. A novel hydrogen-evolving photocatalyst $InVO_4$ active under visible light irradiation. *Chem. Phys. Lett.* 2002; 356:221–226
49. Zhang L, Fu H, Zhang C, Zhu Y. Synthesis, characterization, and photo catalytic properties of $InVO_4$ nanoparticles. *J. Solid State Chem.*, 2006; 179:804–811.
50. Mahapatra S, Nayak KS, Madras G, Guru Row NT. Microwave synthesis and photocatalytic activity of nano lanthanide (Ce, Pr, and Nd) orthovanadates. *Ind. Eng. Chem. Res.* 2008; 47:6509–6516.
51. Tang J, Zou Z, Ye, J. Photocatalytic decomposition of organic contaminants by Bi_2WO_6 under visible light irradiation. *Catal. Lett.* 2004; 92:53–56.

52. Amano F, Yamakata A, Nogami K, Osawa M, Ohtani B. Visible light responsive pristine metal oxide photocatalyst: enhancement of activity by crystallization under hydrothermal treatment. *J. Am. Chem. Soc.*, 2008; 130:17650–17651.
53. Ren J, Wang W, Zhang L, Chang J, Hu S. Photocatalytic inactivation of bac teria by photocatalyst Bi_2WO_6 under visible light. *Catal. Commun.*, 2009; 10:1940–1943.
54. Alfaro OS, Cruz LMA, Torres-Martinez Ma, Lee WS. Remove of marine plankton by photocatalysts with Aurivillius-type structure. *Catal. Commun.*, 2010; 11:326–330.
55. Yu QJ, Kudo A. Hydrothermal synthesis and photocatalytic property of 2-dimensional bismuth molybdate nanoplates. *Chem. Lett.*, 2005; 34:1528–1529.
56. Bi J, Wu L, Li J, Li HZ, Wang XX, Fu ZX. Simple solvothermal routes to syn thesize nanocrystalline Bi_2MoO_6 photocatalysts with different morphologies. *Acta Mater.,* 2007; 55:4699–4705.
57. Zhao X, Xu T, Yao W, Zhu Y. Photodegradation of dye pollutants catalyzed by -Bi_2MoO_6 nanoplate under visible light irradiation. *Appl. Surf. Sci.*, 2009; 255:8036–8040.
58. Zhou L, Wang ZW, Zhang SL. Ultrasonic-assisted synthesis of visible-light induced Bi_2MoO_6 (M = W, Mo) photocatalysts. *J. Mol. Catal. A*. 2007; 268:195–200.
59. Zheng Y, Duan F, Wu J, Liu L, Chen M, Xie Y. Enhanced photocatalytic activ ity of bismuth molybdates with the preferentially exposed {0 1 0} surface under visible light irradiation. *J. Mol. Catal. A*, 2009; 303:9–14.
60. Zhao X, Zhu Y. Synergetic degradation of rhodamine B at a porous ZnWO4 film electrode by combined electro-oxidation and photocatalysis. *Environ. Sci. Technol.*, 2006; 40:3367–3372.
61. Fu, H., Pan, C., Zhang, L., Zhu, Y. Synthesis, characterization and photocatalytic properties of nanosized Bi_2WO_6, $PbWO_4$ and $ZnWO_4$ catalysts. *Mat. Res. Bull.*, 2007, 42, 696–706.
62. Fu H, Lin J, Zhang L, Zhu Y. Photocatalytic activities of a novel $ZnWO_4$ catalyst prepared by a hydrothermal process. *Appl. Catal. A: Chem.*, 2006; 306:58–67.
63. Huang G, Zhu Y. Synthesis and photocatalytic performance of $ZnWO_4$ catalyst. *Mater. Sci. Eng. B*, 2007; 139:201–208.
64. Zhao X, Yao W, Wu Y, Zhang S, Yang H, Zhu Y. Fabrication and photoelec trochemical properties of porous $ZnWO_4$ film. *J. Solid State Chem.*, 2006; 179:2562–2570.
65. Luan J, Zou Z, Lu M, Zheng S, Chen Y. Growth, structural and photophysical properties of Bi_2GaTaO_7. *J. Cryst. Growth*, 2004; 273:241–247.
66. Luan J, Hao X, Zheng S, Luan G, Wu X. Structural, photophysical and pho tocatalytic properties of Bi_2MTaO_7 (M = La and Y). *J. Mater. Sci.* 2006; 41:8001–8012.
67. Luan J, Zou Z, Lu M, Luan G, Chen Y. Structural and photocatalytic properties of the new solid photocatalyst In_2BiTaO_7. *Res. Chem. Intermed.*, 2006; 32:31–42.
68. Luan J, Zheng S, Hao X, Luan G, Wu X, Zou Z. Photophysical and photocat alytic properties of novel M_2BiNbO_7 (M = In and Ga). *J. Braz. Chem. Soc.* 2006, 17:1368–1376.
69. Luan J, Cai H, Zheng S, Hao X, Luan G, Wu X, Zou Z. Structural and photocatalytic properties of novel Bi_2GaVO_7. *Mater. Chem. Phys.* 2007; 104:119–124.
70. Luan J, Cai H, Hao X, Zhang J, Luan G, Wu X, Zou Z. Structural characteri zation and photocatalytic properties of novel Bi_2FeVO_7. *Res. Chem. Intermed.*, 2007; 33:487–500.
71. Luan J, Zhao W, Feng J, Cai H, Zheng Z, Pan B, Wu, X Zou Z, Li Y. Structural, photophysical and photocatalytic properties of novel Bi_2AlVO_7. *J. Hazard. Mater.* 2009; 164:781–789.
72. Luan J, Pan B, Paz Y, Li Y, Wu X, Zou Z. Structural, photophysical and photocatalytic properties of new Bi_2SbVO_7 under visible light irradiation. *Phys. Chem. Chem. Phys.*, 2009; 11:6289–6298.
73. Luan J, Zhang L, Ma K, Li, Y, Zou Z. Preparation and property characterization of new Y_2FeSbO_7 and In_2FeSbO_7 photocatalysts. *Solid State Sci.* 2011; 13:185–194.
74. Luan J, Li M, Ma K, Li Y, Zou Z. Photocatalytic activity of novel Y_2InSbO_7 and Y_2GdSbO_7 nano-catalysts for degradation of environmental pollutant rhodamine B under visible light irradiation. *Chem. Eng. J.*, 2011; 167:162–171.
75. Luan J, Lu M, Zheng S, Zou Z. Optical, structural and photophysical properties of Ga_2BiTaO_7 compound. *J. Mater. Sci.*, 2005; 40:4905–4909.
76. Luan J, Ma K, Pan B, Li Y, Wu X, Zou Z. Synthesis and catalytic activity of new Gd_2BiSbO_7 and Gd_2YSbO_7 nano-catalysts. *J. Mol. Catal. A: Chem.* 2010; 321:1–9.
77. Luan J, Zheng Z, Cai H, Wu X, Luan G, Zou Z. Structural characterization and photocatalytic properties of novel Bi_2YVO_8. *Mater. Res. Bull.*, 2008; 43:3332–3344.
78. Kako T, Zou Z, Ye J. Photocatalytic oxidation of 2-propanol in the gas phase over cesium bismuth niobates under visible light irradiation. *Res. Chem. Intermed.*, 2005; 31:359–364.
79. Kim GH, Hwang WD, Lee SJ. An undoped, single-phase oxide photocatalyst working under visible light. *J Am. Chem. Soc.*, 2004; 126:8912–8913.
80. Kako T, Ye J. Photocatalytic decomposition of acetaldehyde over rubidium bismuth niobates under visible light irradiation. *Mater. Trans.* 2005; 46:2699–2703.
81. Muktha B, Priya HM, Madras G, Guru Row NT. Synthesis, structure, and photocatalysis in a new structural variant of the aurivillius phase: $LiBi_4M_3O_{14}$ (M = Nb, Ta). *J Phys. Chem. B*, 2005; 109:11442–11449.
82. Hatakeyama T, Takeda S, Ishikawa F, Ohmura A, Nakayama A, Yamada Y, Matsushita, A., Ye, J. Photocatalytic activities of Ba_2RBiO_6(R = La, Ce, Nd, Sm, Eu, Gd, Dy) under visible light irradiation. *J. Ceram. Soc. Jpn.* 2010; 118:91–95.
83. Garza-Tovar LL, Torres-MartInez ML, Bernal RodrIguez D, Gomez R, Angel DG. Photocatalytic degradation of methylene blue on Bi_2MNbO_7 (M = Al, Fe, In, Sm) sol–gel catalysts. *J. Mol. Catal. A: Chem.*, 2006; 247:283–290.
84. Torres-Martinez ML, Juarez-Ramirez I, Ramos-Garza SJ, Vazquez-Acosta F, Lee WS. Sol-gel preparation of Bi_2InTaO_7 and its photocatalytic behavior for organic compounds degradation. *Mater. Sci. Forum*, 2010; 658:491–494.
85. Li X, Ouyang S, Kikugawa N, Ye J. Novel Ag_2ZnGeO_4 photocatalyst for dye degradation under visible light irradiation. *Appl. Catal. A: Gen.*, 2008; 334:51–58.

86. Lin X, Huang T, Huang F, Wang W, Shi J. Photocatalytic activity of a Bi-based oxychloride Bi_4NbO_8Cl. *J. Mater. Chem.* 2007; 17:2145–2150.
87. Lin X, Shan Z, Li K, Wang W, Yang J, Huang F. Photocatalytic activity of a novel Bi-based oxychloride catalyst $Na_{0.5}Bi_{1.5}O_2Cl$. *Solid State Sci.* 2007; 9:944–949.
88. Shan Z, Wang W, Lin X, Ding H, Huang F. Photocatalytic degradation of organic dyes on visible-light responsive photocatalyst $PbBiO_2Br$. *J. Solid State Chem.* 2008; 181:1361–1366.
89. Adeel M, Saeed M, Khan I, Muneer M, Akram N. Synthesis and characterization of Co-ZnO and evaluation of its photocatalytic activity for photodegradation of methyl orange. *ACS Omega*. 2021; 6:1426-1435. https://doi.org/10.1021/acsomega.0c05092
90. Saeed M, Usman M, Muneer M, Akram N, Haq A, Tariq M, Akram F. Synthesis of Ag-Fe_3O_4 nanoparticles for degradation of methylene blue in aqueous medium. *Bull. Chem. Soc. Ethiopia.* 2020; 34:123–134. https://doi.org/10.4314/BCSE. V34I1.11
91. Saeed M, Adeel S, Abdur-Raoof H *et al*. ZnO catalyzed degradation of methyl orange in aqueous medium. *Chiang Mai J. Sci.*, 2017; 44:1646–1653. 10.13140/rg.2.2.17237.01762
92. Saeed M, Adeel S, Shahzad MA *et al*. Pt/Al_2O_3 catalyzed decolorization of rhodamine B dye in aqueous medium. *Chiang Mai J. Sci.*, 2015; 42:730–744
93. Umar IG, Halim AA. Heterogeneous photocatalytic degradation of organic contaminants over titanium dioxide: a review of fundamentals, progress and problems. *J. Photochem. Photobiol C: Photochem. Rev.*, 2007; 9:1–12
94. Saeed M, Muneer M, Khosa MKK, Akram N, Khalid S, Adeel M, Nisar A, Sherazi S. Azadirachta indica leaves extract assisted green synthesis of Ag-TiO_2 for degradation of methylene blue and rhodamine B dyes in aqueous medium. Green Processing and Synthesis. 2019; 8:659–666. https://doi.org/10.1515/gps-2019-0036
95. Siddique M, Khan NM, Saeed M. Photocatalytic activity of bis muth ferrite nanoparticles synthesized via sol-gel route. *Zeitschrift fur Physikalische Chemie*, 2019; 233:595–607. https://doi.org/10.1515/zpch-2018-1225
96. Nisar A, Saeed M, Muneer M, Usman M, Khan I. Synthesis and characterization of ZnO decorated reduced graphene oxide (ZnO rGO) and evaluation of its photocatalytic activity toward photodegradation of methylene blue. *Environ. Sci. Poll. Res.* 2021, https://doi.org/10.1007/s11356-021-13520-6
97. Zangeneh H, Zinatizadeh AAL, Habibi M, Akia M, HasnainIsa M. Photocatalytic oxidation of organic dyes and pollutants in wastewater using different modified titanium dioxides: a comparative re view. *J. Ind. Eng. Chem.* 2015; 26:1–36. https://doi.org/10.1016/j.jiec.2014.10.043
98. Lü W, Chen J, Wu Y, Duan L, Yang Y, Ge X. Graphene-enhanced visible-light photocatalysis of large-sized CdS particles for waste water treatment. *Nanoscale Res. Lett.*, 2014; 9:1–7. https://doi.org/10.1186/1556-276X-9-148
99. Ajmal A, Majeed I, Malik RN, Idriss H, Nadeem MA. Principles and mechanisms of photocatalytic dye degradation on TiO_2 based photocatalysts: a comparative overview. *RSC Advances*, 2014; 4:37003-37026. https://doi.org/10.1039/c4ra06658h
100. Muruganandham M, Swaminathan M. TiO_2-UV photocatalytic oxidation of Reactive Yellow 14: effect of operational parameters. *J. Hazard. Mater.*, 2006; 135:78–86. https://doi.org/10.1016/j.jhazmat.2005.11.022
101. Kumar D, Ameta R. Use of photo-Fenton reagent for the degradation of basic orange 2 in aqueous medium. *J. Chem. Pharm. Res.*, 2013; 5(1):68-74.
102. Kusic H, Koprivanac N, Horvat S, Bakija S, Bozic AL. Modeling dye degradation kinetic using dark and photo-Fenton type processes. *Chem. Eng. J.*, 2009; 155(1-2):144-154.
103. Garcia-Montano J, Domenech X, Garcia-Hortal JA, Torrades F, Peral J. The testing of several biological and chemical coupled treatments for Cibacron Red FN-R azo dye removal. *J. Hazard. Mater.*, 2008; 154(1-3):484-490.
104. Zheng H, Pan Y, Xiang X. Oxidation of acidic dye eosin Y by the solar photo-Fenton processes. *J Hazard. Mater.*, 2007; 141(3):457-464.
105. Sun JH, Sun SP, Wang GL, Qiao LP. Degradation of azo dye amido black 10B in aqueous solution by Fenton oxidation process. *Dyes Pigments*, 2007; 74(3):647-652.
106. Daneshvar N, Khataee AR. Removal of azo dye C.I. acid red 14 from contaminated water using Fenton, UV/H_2O_2, UV/H_2O_2/Fe(II), UV/H_2O_2/Fe(III) and UV/H_2O_2/Fe(III)/oxalate processes: A comparative study. J. Environ. Sci. Health A Toxicol. *Hazard. Subst. Environ. Eng.*, 2006; 41(3):315-328.
107. Zheng HL, Xiang XY. Photo-Fenton oxidation processes used in the degradation of rhodamine B. Guangpu, 2004; 24(6):726-729.
108. Neamtu M, Yediler A, Siminiceanu I, Kettrup A. Oxidation of commercial reactive azo dye aqueous solutions by the photo-Fenton and Fenton-like processes. *J. Photochem. Photobiol. A Chem.*, 2003; 161(1):87-93.
109. Xie Y, Chen F, He J, Zhao J, Wang H. Photo-assisted degradation of dyes in the presence of Fe and H_2O_2 under visible irradiation. *J. Photochem. Photobiol. A: Chem.*, 2000; 136(3):235-240.
110. Wu K, Xie Y, Zhao J, Hidaka H. Photo-Fenton degradation of a dye under visible light irradiation. *J. Mol. Catal. A: Chem.,* 1999; 144(1):77-84.
111. Alalm MG, Tawfik A, Ookawara S. Comparison of solar TiO_2 photocatalysis and solar photo-Fenton for treatment of pesticides industry wastewater: operational conditions, kinetics, and costs. *J. Water Proc. Eng.* 2015; 8:55-63.
112. Dbira S, Bedoui A, Bensalah N. Investigations on the degradation of triazine herbicides in water by photo-Fenton process. *Am. J. Anal. Chem.*, 2014; 5(8):500-517.
113. Sanchez, J.A., Roman, I.M., Carra, I., Cabrera, A., Casas, J.L., Malato, S. Economic evaluation of a combined photo-Fenton/MBR process using pesticides as model pollutant, Factors affecting costs. *J. Hazard. Mater.*, 2013; 244-245:195-203.
114. Vilar VJP, Moreira FC, Ferreira ACC, Sousa MA, Goncalves C, Alpendurada MF *et al*. Biodegradability enhancement of a pesticide-containing bio-treated wastewater using a solar photo-Fenton treatment step followed by a biological oxidation process. *Water Res.*, 2012; 46(15):4599-4613.
115. Karale R, Manu SB, Shrihari S. Fenton and photo-Fenton oxidation processes for degradation of 3 aminopyridine from water. *APCBEE Proc.* 2014; 9:25-29.
116. Farre MJ, Franch MI, Malato S, Ayllon JA, Peral J, Domenech X. Degradation of some biorecalcitrant pesticides by homogeneous and heterogeneous photocatalytic ozonation. *Chemosphere*, 2005; 58(8):1127-1133.

117. Derbalah AS, Nakatani N, Sakugawa H. Photocatalytic removal of fenitrothion in pure and natural waters by photo-Fenton reaction. *Chemosphere*, 2004; 57(7):635-644.
118. Orbeci C, Untea I, Nechifor G, Segneanu AE, Craciun ME. Effect of a modified photo-Fenton proc dure on the oxidative degradation of antibiotics in aqueous solutions. *Sep. Purif. Technol.*, 2014; 122:290-296.
119. Batista APS, Nogueira RFP. Parameters affecting sulfonamide photo-Fenton degradation-iron complexation and substituent group. *J. Photochem. Photobiol. A Chem.*, 2012; 232(15):8-13.
120. Perez-Moya M, Graells M, Castells G, Amigo J, Ortega E, Buhigas G *et al*. Characterization of the degradation performance of the sulfamethazine antibiotic by photo-Fenton process. *Water Res.*, 2010; 44(8):2533-2540.
121. Radjenoviæ J, Sirtori C, Petroviæ M, Barcelo D, Malato S. Characterization of intermediate products of solar photocatalytic degradation of ranitidine at pilot-scale. *Chemosphere*, 2010; 79(4):368-376.
122. Giri AS, Golder AK. Fenton, photo-Fenton, H_2O_2 photolysis, and TiO_2 photocatalysis for dipyrone oxidation: drug removal, mineralization, biodegradability, and degradation mechanism. *Ind. Eng. Chem. Res.*, 2014; 53:1351-1358.
123. Karale R, Manu SB, Shrihari S. Fenton and photo-Fenton oxidation processes for degradation of 3 aminopyridine from water. *APCBEE Proc.* 2013; 9:25-29.
124. Alalm MG, Tawfik A, Ookawara S. Degradation of four pharmaceuticals by solar photo-Fenton process: kinetics and costs estimation. *J. Environ. Chem. Eng.* 2015; 3(1):46-51.
125. Elmolla ES, Chaudhuri M. Photo-Fenton treatment of antibiotic wastewater. *Nat. Environ. Pollut. Technol.*, 2010; 9(2):365-370.
126. Baydum VPA, Dantas RF, Teixeira A, Pacheco JGA, Silva VL. Pre-treatment of propranolol effluent by advanced oxidation processes. *Afinidad.* 2012, LXIX 211-216.
127. Sirtori C, Zapata A, Oller I, Gernjak W, Aguera A, Malato S. Decontamination industrial pharmaceutical wastewater by combining solar photo-Fenton and biological treatment. *Water Res.* 2009; 43(3):661-668.